Clays and Clay Minerals, Vol. 39, No. 3, pp. 239–247, 1991.

K-RICH MORDENITE FROM LATE MIOCENE RHYOLITIC TUFFS, ISLAND OF SAMOS, GREECE

G. PE-PIPER[1] AND P. TSOLIS-KATAGAS[2]

[1] Department of Geology, Saint Mary's University
Halifax, Nova Scotia B3H 3C3, Canada

[2] Department of Geology, University of Patras, Patras 261 110, Greece

Abstract—Mordenite occurs in hydrothermally altered rhyolitic volcanic rocks at the margin of a Late Miocene lake basin on the island of Samos, Greece. The mordenite was identified by its X-ray powder diffraction pattern and appearance in scanning electron micrographs. Electron microprobe analyses show high Si, Ca, and K, low Na, and high balance errors. The *b* cell dimension is consistent with a high Si/(Al + Si) ratio, and the balance errors are apparently due to Na deficiency. The missing Na was estimated from the amount required to give (Si + Al) = 48 and yielded analyses comparable with X-ray fluorescence analyses of samples predominantly of mordenite. Even after this correction, the mordenite had a low Na:K ratio compared with most analyses reported in the literature. The peculiar chemistry of the mordenite may have resulted from a high-temperature metasomatic origin as a result of basaltic volcanism at the basin margin and characterized by hydrothermal circulation of alkaline lake water rich in K.

Key Words—Hydrothermal alteration, Mordenite, Potassium, Rhyolitic tuff, Volcanic ash, X-ray powder diffraction, Zeolite.

INTRODUCTION

Rhyolitic tuffs containing the siliceous zeolite mordenite occur at the eastern margin of the Miocene Karlovasi lacustrine basin in the western part of the island of Samos (eastern Aegean Sea). Rhyolitic tuffs, flow-banded rhyolite domes, and small basalt cones crop out at the basin margin, where they are interbedded with Tortonian ash fall tuffs and tuffites. The volcanic rocks are overlain and underlain by calcareous marlstone in the main part of the basin (Meissner, 1976; Stamatakis, 1989a). In the tuffaceous rocks of the basin, diagenetic boron-bearing K-feldspar (Stamatakis, 1989b), clinoptilolite, and analcime show a regular spatial and stratigraphic distribution (Stamatakis, 1989a). Gypsum, celestite, and thenardite are also present and indicate the existence of a saline, alkaline lake.

Mordenite has been synthesized from a variety of starting materials and chemical systems and over a temperature range of about 75°–400°C (Barrer, 1948, 1982; Nakajima, 1973; Seki, 1973; Senderov, 1963; Whittemore, 1972). In volcanic rocks, crystallization of the highly siliceous zeolites, clinoptilolite and mordenite, is favored by a highly silicic composition of original glass (Sheppard *et al.*, 1988) and a pH in the range of 7–9 (Mariner and Surdam, 1970; Sheppard *et al.*, 1988). Mordenite is favored over clinoptilolite by higher temperatures and higher Na:K ratios (Wirsching, 1976; Hawkins *et al.*, 1978; Kirov *et al.*, 1979; Phillips, 1983). Kusakabe *et al.* (1981) showed experimentally that the hydrothermal conversion of clinoptilolite to mordenite required higher temperatures with a decrease in Na^+ concentration or pH. In natural occurrences associated with alkaline lakes, clinoptilolite occurs as a low-temperature alteration of silicic tuffs (Gude and Sheppard, 1988). Authigenic mordenite formed under low-temperature conditions is known from alkaline lakes (Maglione and Tardy, 1971) and has been described from hydrothermally altered rhyolites (Phillips, 1983).

In this study, we describe mordenite of an unusual chemical composition from Samos and account for its presence, rather than clinoptilolite or aluminous zeolites, and its unusual chemistry in the light of experimental work and field studies by others.

GEOLOGIC SETTING

The mordenite occurs in several tens of meters of rhyolitic tuffs and flow-banded rhyolite exposed in road cuts northwest of Koumeika (Figure 1). In the same area, small basalt cones and marls with tufa (indicating hot spring activity) are exposed. The rhyolitic rocks are intensely altered. Much of this alteration has taken place along veins, which are associated with either zeolitization or silicification. Elsewhere, the entire outcrop appears to consist of a green rock that may have originally been perlite, but which is now relatively soft zeolitic material. Volcaniclastic conglomerate immediately overlying the rhyolites contain clasts of both basalt and fresh (dark-gray) flow-banded rhyolite. Stamatakis (1989a) identified mordenite, cristobalite, and tridymite in one sample from these outcrops (sample 103).

We have obtained a new whole-rock K/Ar date of 8.7 ± 0.4 Ma on a rhyolite (sample 77). The adjacent and overlying basalts have yielded ages between 8.3 and 7.8 Ma (Fytikas *et al.*, 1984). This igneous activity

was synchronous with sedimentation in the Karlovassi basin (Stamatakis, 1989a).

ANALYTICAL METHODS

About 30 samples were collected and examined. Selected samples were examined in thin section and by scanning electron microscopy (SEM). The mineralogy of the samples (Table 1) was determined by X-ray powder diffractometer (XRD) analysis, using packed powdered sample, CuKα radiation, and a scan from 2° to 42°2θ at a speed of 0.25°2θ/min. Cell dimensions were determined from XRD patterns. Peak positions and cell parameters were refined using the algorithm of Appleman and Evans (1973).

Representative samples were analyzed for 10 major and minor element oxides and 14 trace elements on a Philips PW1400 sequential X-ray fluorescence spectrometer using a Rh-anode X-ray tube. Major oxide determinations were made on fused glass discs, whereas trace elements were determined from pressed powder pellets. International standards with recommended values from Abbey (1983), as well as in-house standards, were used for calibration. Analytical precision, as determined from replicate analyses, was generally better than 2%, except MgO, Na_2O, and Nb, which were better than 5%, and Th, which was better than 10%. Loss on ignition (LOI) was determined by heating the sample for 1.5 hr at 1050°C in an electric furnace. Chemical analyses of minerals were made with JEOL-733 electron microprobe having four wavelength spectrometers and a Tracor Northern 145-eV energy-dispersive detector. Geological standards were used. The beam was operated with a 5-nA beam current and defocused to 10 to 20 μm during the analysis of zeolites

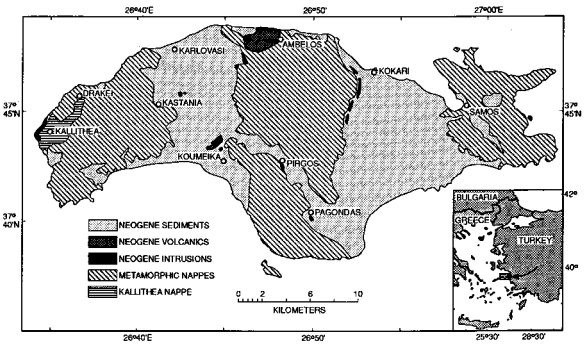

Figure 1. Geological map of Samos, Greece, showing Neogene sedimentary basins. Studied samples came from the large Neogene volcanic outcrop northwest of Koumeika.

Table 1. Mineralogy of altered volcanic rocks from Samos, Greece, as determined by X-ray powder diffraction.[1]

Sample	Mord	Sme	Cr/Tr	Mi	Qtz	Feld	Dol	Cal	Lithology
75	A	P	P	—	—	—	—	—	Tuff
76	A	P	P	—	—	—	—	—	Tuff
77a	—	—	—	—	A	P	—	—	Rhyolite, gray
77b	—	—	—	—	A	P	—	—	Rhyolite, pink
80	A	P	P	—	—	—	—	—	Rhyolite(?)
81	—	—	—	—	A	P	—	—	Rhyolite
82a	—	—	—	—	A	P	—	—	Rhyolite, pink
82b	—	—	—	—	A	P	—	—	Rhyolite, white
83	—	—	—	—	—	—	A	—	Carbonate clast
89a	—	—	—	P-T	A	T	—	A	Tuff
89b	—	—	—	P	A	T	—	?	Tuff
92a	—	—	—	—	A	P	—	—	Rhyolite, gray
92b	—	—	—	—	A	P	—	—	Rhyolite, pink
92c	—	—	—	—	A	P	—	—	Rhyolite, white
93a	—	—	—	—	A	P	—	—	Rhyolite, gray
93b	—	—	—	—	A	P	—	—	Rhyolite, pink
93c	—	—	—	—	P	P	—	—	Rhyolite, white
94a	—	—	—	—	A	P	—	—	Silicified vein, pink
94b	—	—	—	—	A	P	—	—	Silicified vein, gray
95a	—	—	—	—	A	P	—	—	Silicified vein
95b	—	—	—	—	A	P	—	—	Silicified vein
96	A	P	P	—	—	—	—	—	Tuff
97	A	P	P	—	—	—	—	—	Tuff
98	—	—	—	—	P-T	A	—	—	Rhyolite
99	A	P	A	—	—	—	—	—	Rhyolite(?)
100a	—	—	—	—	P	A	—	—	Tuff, gray
100b	—	—	—	—	P-T	A	—	—	Tuff, pink
101	A	T	A	—	—	P	—	—	Tuff, green
101w	A	P	P	—	—	P	—	—	Tuff, white

[1] Mord = mordenite; Sme = smectite; Cr/Tr = cristobalite and tridymite, Mi = mica, Qtz = quartz, Feld = feldspars, Dol = dolomite, Cal = calcite; A = abundant, P = present, T = trace.

https://doi.org/10.1346/CCMN.1991.0390303 Published online by Cambridge University Press

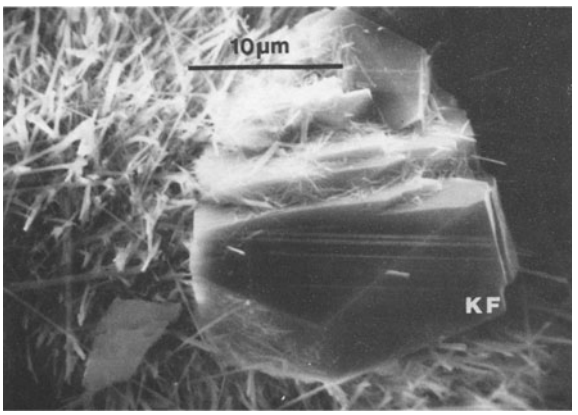

Figure 2. Scanning electron micrograph of sample 99 showing filiform mordenite draped across euhedral K-feldspar (KF).

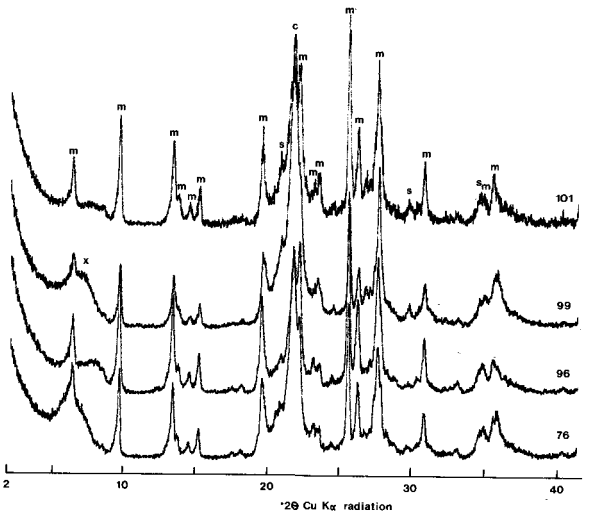

Figure 3. X-ray powder difractograms of untreated samples. M = mordenite, C = cristobalite, S = sanidine, X = smectite.

to prevent loss of volatiles. The data were reduced using a Tracor Northern ZAF matrix correction program.

RESULTS

Petrography

The primary lithologies identified were spherulitic rhyolite and rhyolitic tuff. Both lithologies were rich in a vitric component, either glass shards or devitrified groundmass. Rare pyrogenic K-feldspar (Figure 2) and plagioclase crystals were present in all rocks, and both contained quartz overgrowths. The vitric matrix of the tuffs and some rhyolites was replaced by authigenic minerals. Completely devitrified groundmass consisted of mordenite, smectite, sanidine, tridymite, and cristobalite (Figure 3). Although albite was not detected in diffractograms, electron microprobe analysis of devitrified groundmass indicated a silica mineral, K-feldspar, and albite. Mordenite was the only zeolite in these rocks; clinoptilolite or aluminous zeolites were not found. Samples rich in mordenite were also rich in silica minerals.

Mordenite-free rocks, including both rhyolites and tuffs, were dark gray in hand specimen, with pink or white altered areas. Mordenite-bearing rocks include

Table 2. Representative electron microprobe analyses of mordenite.

Rock sample	75			76			99		101		
Crystal number	1	1B	1B*	1-2	2-2	3	4-1	5	1-1	2-1	2-2
SiO_2	73.02	71.72	71.14	69.68	68.69	72.20	69.91	69.96	70.07	68.22	71.06
Al_2O_3	11.46	10.84	10.89	10.68	10.49	11.43	11.62	11.35	11.11	10.67	11.49
FeO_t	0.11	n.d.	0.07	0.04	0.02	0.16	0.13	0.06	0.11	0.09	0.08
MgO	n.d.	n.d.	0.01	0.03	0.04	n.d.	0.03	0.02	0.01	n.d.	0.01
CaO	3.03	3.13	3.20	3.09	3.18	3.49	3.23	3.18	2.47	2.90	3.27
Na_2O (meas.)	0.77	0.77	0.93	1.20	1.15	0.79	1.29	1.54	0.51	0.69	1.23
Na_2O (calc.)	1.90	2.11	2.13	1.83	1.68	1.89	2.33	2.37	1.84	2.12	1.89
K_2O	2.45	1.55	1.30	1.79	1.64	1.66	1.50	1.40	3.12	1.63	2.14
Formula on the basis of 96(O) using recalculated Na_2O content											
Si	40.51	40.74	40.67	40.65	40.68	40.44	40.14	40.30	40.45	40.53	40.31
Al	7.50	7.26	7.34	7.35	7.33	7.55	7.87	7.71	7.56	7.47	7.69
Fe	0.05	0.00	0.03	0.02	0.01	0.08	0.06	0.03	0.05	0.05	0.04
Mg	0.00	0.00	0.01	0.03	0.04	0.00	0.03	0.02	0.01	0.00	0.01
Ca	1.80	1.91	1.96	1.93	2.02	2.10	1.99	1.96	1.53	1.85	1.99
Na (calc.)	2.04	2.32	2.36	2.07	1.93	2.05	2.59	2.65	2.06	2.44	2.08
K	1.73	1.12	0.95	1.33	1.24	1.19	1.10	1.03	2.30	1.24	1.55
E% (meas. Na_2O)	22	25	24	11	9	24	19	14	35	37	15
E% (calc. Na_2O)	2.3	0.4	2.0	1.4	1.2	2.6	2.5	1.3	2.4	2.0	0.8

n.d. = not detected. All analyses performed with defocussed beam except *, which was by scanning beam. Na_2O (calc.) is based on adding Na_2O to make Si + Al = 48.0.

https://doi.org/10.1346/CCMN.1991.0390303 Published online by Cambridge University Press

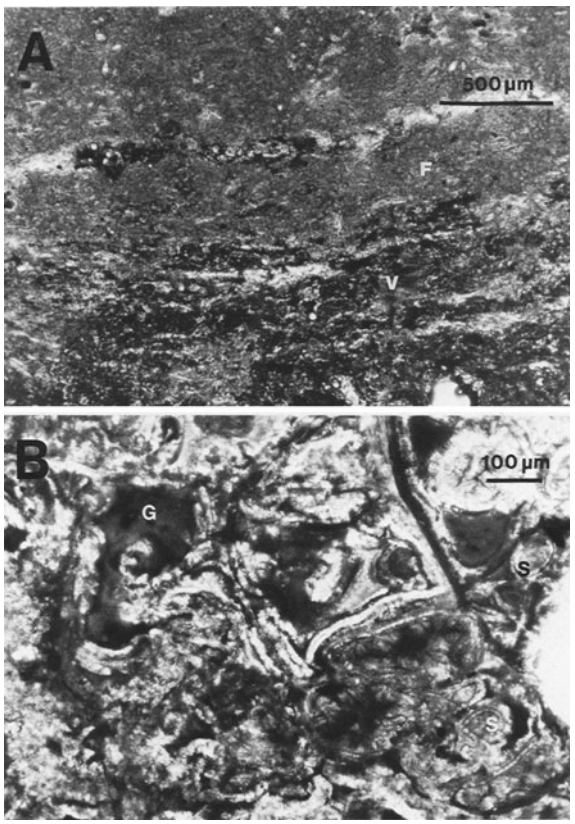

Figure 4. Photomicrographs of banded tuff (sample 101, plane polars). A = Alternating bands of mordenite-rich vitric tuff (V) and fine-grained matrix with normal spherulites (F). B = The vitric band at higher magnification. Mordenite occurs as spherulites (S) and as pseudomorphs after glass shards (G).

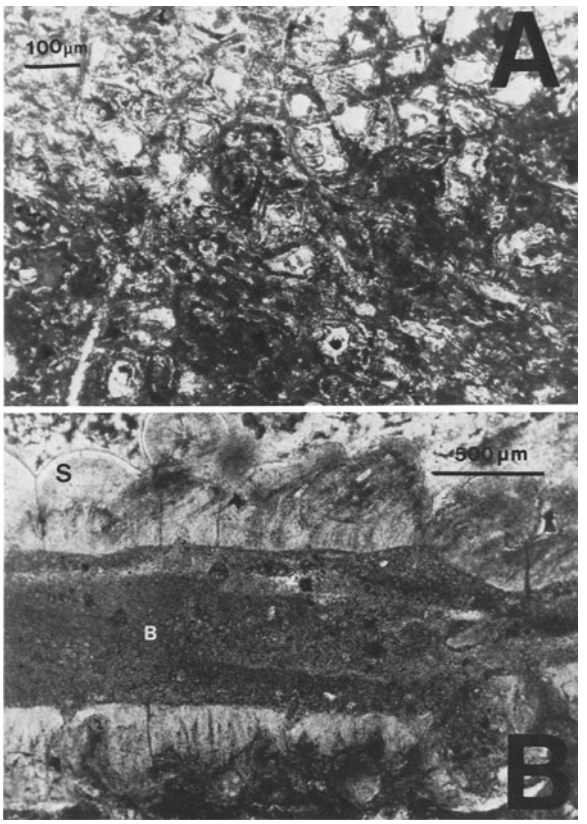

Figure 5. Photomicrographs of tuff with spherulites and bands of quartzo-feldspathic composition (sample 99, plane polars). A = Fine-grained vitric tuff rich in mordenite. B = Band cutting the tuff (B) rimmed by spherulites (S).

flow-banded rhyolites and whitish-green tuffs. Some samples (originally tuff or perlite) consisted of bands having "normal" (quartz-feldspar) spherulites of various shapes set in a very fine-grained matrix (Figure 4A) alternating with areas of vitroclastic texture having relict glass shards now replaced by mordenite (Figure 4B). In some vitreous pyroclastic rocks (Figure 5), the normal spherulites were organized in laminae, which may reflect a primary flow banding or bedding (Figure 4A). In the spherulitic rhyolites, all spherulites were set in a devitrified, fine-grained matrix. Some tuffs contained irregular cavities as large as 3 mm in diameter, which were bounded by irregular bands of mordenite spherules.

Spherulites include those of mordenite and those of quartzo-feldspathic composition. The latter, referred to as normal spherulites, were most common. They had a thin clear margin (Figure 6) of K-feldspar and a dusty-looking gray core of K-feldspar and quartz, which was browner towards the center (Figure 6B). Some such spherulites apparently nucleated around K-feldspar phenocrysts (Figure 6A).

Description of mordenite

Mordenite was readily identified in thin section by its brown color and fibrous habit, which was also distinctive in scanning electron micrographs. The identification was confirmed by electron microprobe analyses and by XRD.

The most common occurrence of mordenite was as fibrous brown spherulites (generally as large as 100 μm) that occurred as isolated masses (Figure 7A), in clusters (Figure 7B), or as pseudomorphed glass shards (Figure 8A). Such pseudomorphed shards showed a central hollow zone, a gray intermediate zone, and a rim of brownish spherulites, some of the which had a very thin clear rim (Figure 8A). Both the gray intermediate zone and the thin rims of the spherulites yielded chemical analyses similar to mordenite, but had lower totals than other analyses. Mordenite also occured in bands rimming cavities (Figure 8B).

Some spherulites in sample 99 showed an apparent transition from quartzo-feldspathic to mordenite composition. The mordenite occurred as fibrous crystals

https://doi.org/10.1346/CCMN.1991.0390303 Published online by Cambridge University Press

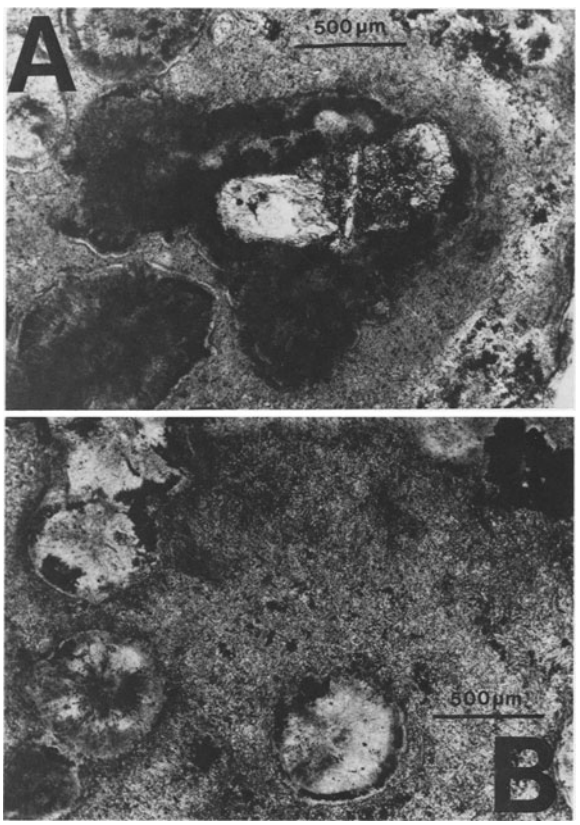

Figure 6. Photomicrographs of relatively fresh spherulitic rhyolite without zeolite. In A, spherulites grew around feldspar phenocrysts. In A and B, the clear rim around the normal spherulites is visible. Sample 77, plane polars.

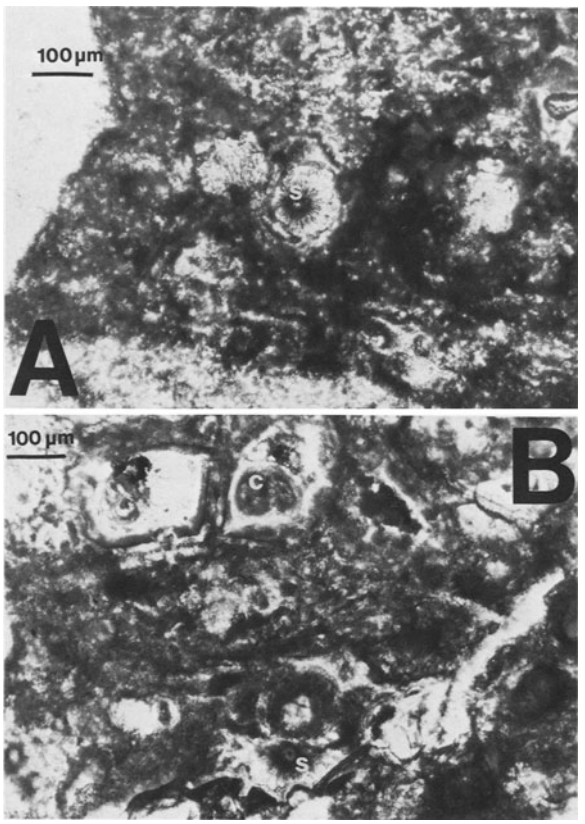

Figure 7. Photomicrographs of mordenite-rich bands in banded tuff (sample 99, plane polars). Mordenite occurs as isolated spherulites (S) or in clusters (C) in both A and B.

on the outer part of the clear quartzo-feldspathic rim and second-order spherulites that lined the hollow gray core (Figure 9). Mordenite also occured as yellowish fibrous aggregates, about 70 × 30 μm in size, dispersed through the rock and as filiform material draped across earlier smectite (Figure 10).

Chemical composition of mordenite

Mordenite crystals from four samples were analyzed by electron microprobe (Table 2). Compared with mordenite samples from elsewhere (Passaglia, 1975; Gottardi and Galli, 1985), they had very low Na_2O and rather high (Si + Al) contents, with a mean value of 48.25 for 96 oxygen atoms, compared with a theoretical value of 48.00 (Gottardi and Galli, 1985). Furthermore, the balance error (E = 100[(Al + Fe) − (Na + K) − 2(Mg + Ca)]/[(Na + K) + 2(Mg + Ca)]) in most samples was between 14 and 25%, consistently higher than the accepted value of <10% (Gottardi and Galli, 1985).

Passaglia (1975) showed that the *b* cell dimension of mordenite varies systematically with the Si/(Al + Si) ratio. Estimated *b* cell dimensions were between 20.44 to 20.46, with standard errors on individual determinations being <0.005. The Appleman and Evans (1973) algorithm requires input of estimates of the *b* dimension: the estimate of refined *b* dimension was unchanged for initial estimates ranging from 20.40 to 20.52 (the natural range reported by Passaglia, 1975). Samples of the Samos mordenite had nearly constant Si/(Al + Si) ratios of 0.84 and mean *b* dimensions of 20.45 Å, corresponding closely to the values found by Passaglia (1975) for mordenite samples having low balance errors. Thus, the balance error probably was not due to high Al; rather, it resulted from relatively low exchangeable cations. The very low Na_2O content suggests that this was principally due to low Na.

The quantity of Na_2O required to make the sum of Si and Al framework constituents equal to the theoretical and empirically confirmed value of 48.0 was calculated (Table 2). Balance errors using these calculated Na_2O values are ≤2.6, suggesting that Na was mobilized and/or volatilized under the electron beam. To evaluate this effect, replicate electron microprobe analyses were made using both spot and scanning techniques, with various sizes of the defocussed beam.

https://doi.org/10.1346/CCMN.1991.0390303 Published online by Cambridge University Press

Table 3. X-ray fluorescence analyses of altered volcanic rocks from Samos.

Sample	100a	100b	92a	92b	93a	93b	77a	77b	79	78	101	97	96
	Samples lacking mordenite										Samples with mordenite		
	Tuff		Glassy rhyolite		Sph. rhyolite		Sph. rhyolite		Rhyolite	Rhyolite	Tuff	Tuff	Tuff(?)
	Gray	Pink	Gray	Pink	Gray	Pink	Gray	Pink	Gray	White	Green	*Lt Green*	Lt green
	Major elements (wt. %)												
SiO_2	78.70	78.27	77.99	78.28	77.60	77.62	77.09	77.34	77.06	74.97	74.56	71.13	70.42
TiO_2	0.06	0.06	0.05	0.06	0.06	0.06	0.06	0.06	0.06	0.07	0.06	0.06	0.07
Al_2O_3	11.17	11.72	11.67	11.89	12.40	12.30	12.08	12.38	12.88	13.78	10.56	11.77	12.61
Fe_2O_{3t}	0.54	0.43	0.61	0.57	0.43	0.81	0.72	0.46	0.35	0.30	0.92	1.07	1.32
MnO	0.02	0.01	0.01	0.01	0.01	0.01	0.01	0.01	0.01	0.01	0.03	0.03	0.03
MgO	0.71	0.80	0.64	0.69	0.71	0.75	0.79	0.71	0.77	0.90	0.99	1.18	0.99
CaO	0.16	0.26	0.04	0.04	0.07	0.09	0.07	0.06	0.10	0.16	1.49	1.47	1.85
Na_2O	3.51	3.81	2.57	1.70	3.22	2.79	2.44	2.57	3.51	2.71	1.10	1.50	1.51
K_2O	4.01	4.14	6.32	6.71	5.88	5.85	6.24	6.93	5.08	6.14	3.35	3.02	2.85
P_2O_5	0.01	0.01	0.01	0.01	0.01	0.01	0.01	0.01	0.01	0.01	0.01	0.01	0.01
L.O.I.	1.00	1.10	1.00	0.70	0.60	0.70	1.10	0.60	0.90	1.80	8.00	9.70	10.00
Total	99.89	100.61	100.91	100.66	100.99	100.99	100.61	101.13	100.73	100.85	101.07	100.94	101.66
	Trace elements (ppm)												
Ba	<5	7	25	15	13	10	11	10	8	7	8	15	27
Rb	295	279	503	494	437	432	456	502	328	311	597	708	710
Sr	26	55	<5	5	23	<5	<5	<5	9	7	366	313	443
Y	38	34	53	49	37	37	50	52	42	44	46	59	80
Zr	136	144	138	127	132	129	136	135	164	169	142	156	166
Nb	94	77	67	62	62	70	67	66	63	61	63	70	72
Th	<10	<10	<10	<10	<10	<10	<10	<10	<10	<10	<10	<10	<10
Pb	48	34	12	30	<10	<10	34	33	26	59	57	53	<10
Ga	15	17	17	18	18	16	17	18	18	20	16	18	19
Zn	29	19	42	18	10	13	66	22	15	17	48	53	60
Cu	<5	<5	10	8	<5	7	7	5	<5	<5	<5	<5	<5
Ni	5	<5	<5	<5	<5	<5	<5	<5	<5	<5	<5	<5	<5
V	<5	<5	<5	<5	<5	<5	<5	<5	<5	<5	<5	<5	<5
Cr	15	11	13	12	11	11	12	9	10	10	11	8	11

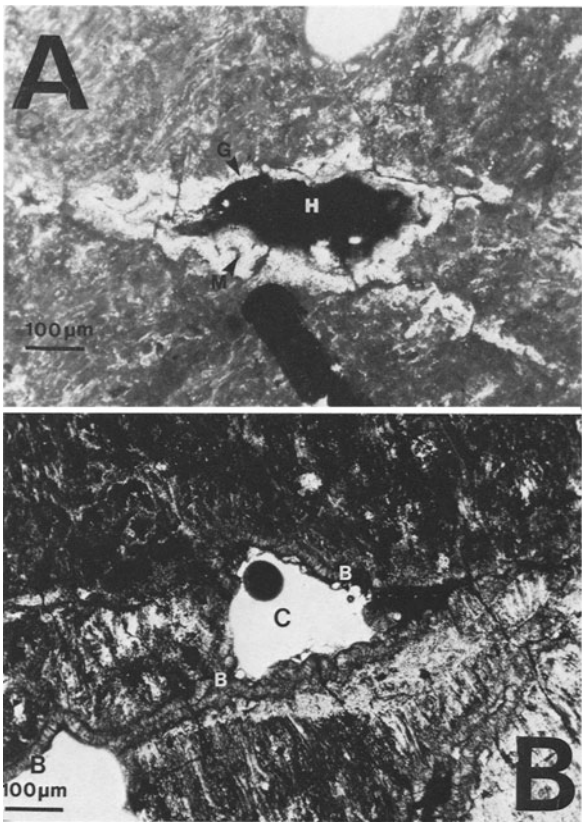

Figure 8. Photomicrographs of mordenite-rich tuffs. A = Pseudomorph of shard is defined by several layers of mordenite spherulites. The pseudomorph is hollow (H), rimmed by gray mordenite(?) (G) and brown mordenite spherulites (M). Sample 76, plane polars. B = small bands of mordenite spherulites (B) that rim a cavity (C). Sample 75, plane polars.

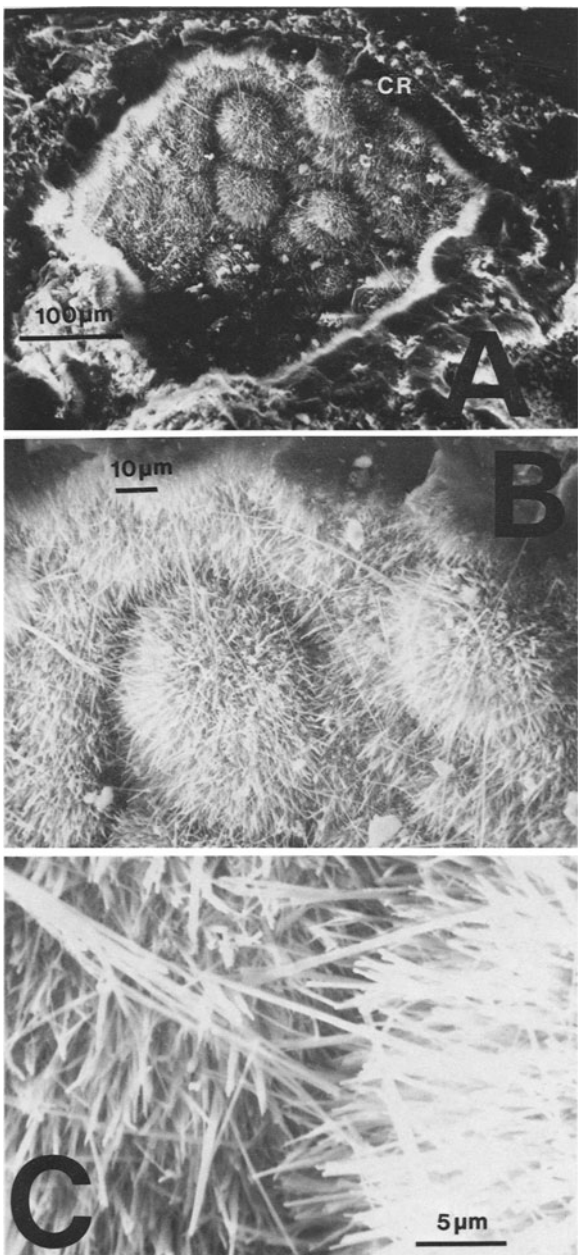

Figure 9. Scanning electron micrograph of sample 99 (tuff) showing mordenite lining the internal walls of the hollow core of a broken normal spherulite. A to C are successive enlargements of the same position. Note the spherulitic and filiform development of the mordenite. CR = clear rim.

Analyses of any particular crystal by the various methods were reasonably consistent, although variations of as much as 0.2% Na_2O were common. Sheppard *et al.* (1988) also found low totals and low Na in microprobe analyses of mordenite from Yucca Mountain, Nevada. The XRF analyses of predominantly mordenitic samples (96, 97, and 101 in Table 3) provide some independent assessment of mordenite composition. These samples also contained minor sanidine, smectite, and cristobalite. Overall, these samples contained about twice as much K_2O as Na_2O.

Using the calculated Na_2O values, the average Na:K ratio is 1.66. If the exchangeable cation deficiency was in part due to K, rather than Na, then this ratio would be even lower. The potassium content of these mordenites is unusually high compared with analyses summarized by Gottardi and Galli (1985) (average Na:K = 8.61) and Passaglia (1975) (average Na:K = 8.93). It is comparable with two analyses reported by Sheppard *et al.* (1988) from Yucca Mountain (Na:K = 0.57 and 2.19). The average Na:K ratio of the predominantly mordenite whole-rock samples was 0.68, lower than the calculated microprobe analyses, principally as a result of sanidine contamination.

We thus conclude that the Samos mordenite has an unusually low Na:K ratio compared with most mordenite analyses in literature, and the recalculated compositions in Table 2 are reasonable estimates of actual composition.

https://doi.org/10.1346/CCMN.1991.0390303 Published online by Cambridge University Press

DISCUSSION

Chemical changes during zeolitization

Chemical analyses of bulk samples of rhyolitic rocks are given in Table 3. Analyses 101, 97, and 96 are of mordenite-rich samples; the remainder are of mordenite-free samples. Although sample 78 contained no mordenite, it was more altered than the other mordenite-free samples. In general, pink rocks were more altered than gray rocks. Analyses of areas of different colors in the same sample (Table 3) show that with progressive change from gray to pink to white, K_2O tends to increase; other chemical changes are not large.

Much larger differences exist between mordenite-free and mordenite-rich samples. If mordenite-rich samples originally resembled mordenite-free samples, a measure of gains and losses of chemical components during metasomatism is provided. The mordenite-bearing rocks contained lower concentrations of alkalis and significantly higher concentrations of FeO_t, MgO, CaO, LOI, Rb, and Sr. The FeO_t and MgO were presumably held principally in smectite; CaO and Sr were principally in mordenite. The site of the Rb is uncertain. Similar changes have been noted in the Miocene silicic tuffs at Yucca Mountain (Sheppard *et al.*, 1988) and in the diagenetic alteration of silicic glass to mainly clinoptilolite in the John Day Formation of Oregon (Hay, 1963) and the Ricardo Formation of California (Sheppard and Gude, 1965).

Genesis of the Samos mordenite

Alteration of the rhyolitic flows and tuffs in this region is associated with discrete veins and fractures, suggesting that the alteration was influenced by fluid flow. The presence of nearby hot spring tufa is consistent with this interpretation. Smectite was apparently the first mineral to crystallize, and it occurs in samples that do not contain mordenite. In samples rich in mordenite, the filiform mordenite drapes across smectite. The early formation of smectite was probably favored by a relatively low $(Na^+ + K^+)/H^+$ activity ratio in the pore fluid (Hemley, 1962). Continuing alteration of glass to smectite would have raised the pH, a_{SiO_2}, and $(Na^+ + K^+)/H^+$ activity ratio, providing a chemical environment favorable for the formation of mordenite. Samples rich in mordenite are also enriched in silica minerals, suggesting that at the time mordenite formed, excess silica was present and was precipitated. Mordenite rims holes and occurs in bands throughout the rocks, which suggests a formation by the dissolution of glass involving flow through the resulting porous rocks.

Although the parent rhyolites are siliceous, their silica content is not particularly high compared with other rhyolites from which mordenite has been reported. They are also rich in K_2O relative to Na_2O, so that the dissolution of such glasses should not have produced solutions with high Na:K ratios. Indeed, clinoptilolite rather than mordenite should have formed if the pore water were derived from the rhyolites.

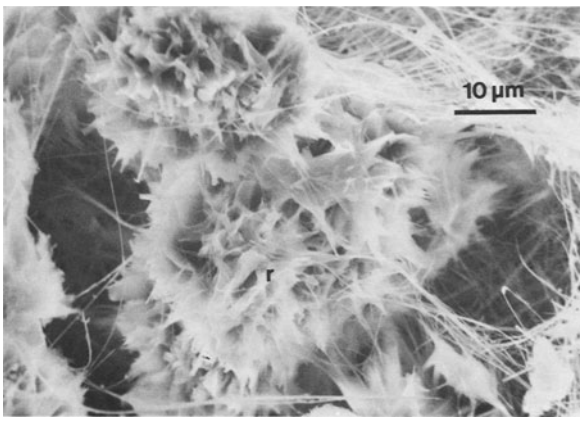

Figure 10. Scanning electron micrograph of sample 99 showing a tangle of filiform mordenite draped across authigenic smectite.

The concentration of much of the pre-mordenite alteration along major fractures and the scale of the metasomatic alteration suggest substantial transport of chemical species in a hydrothermal circulation system. The presence of such hydrothermal circulation is also indicated by the tufa deposits.

Several studies (e.g., Sheppard *et al.*, 1988; Barth-Wirsching and Höller, 1989) have indicated that relatively high temperatures favor mordenite formation. In Samos, the basaltic volcanism that followed the extrusion of rhyolite occurred at the margin of the lake basin. This basaltic heat source could have driven a substantial high-temperature hydrothermal circulation. The alkaline lake would have provided the principal source of water for hydrothermal recharge. The composition of the sediments in the Karlovassi basin indicates that the resulting hydrothermal waters could have had high K and Ca contents. Chemical analyses of the marls in the Hora Formation in the Mytilini basin of eastern Samos have substantially higher amounts of K_2O than Na_2O (Stamatakis and Zagouroglou, 1984). The experimental work of Kusakabe *et al.* (1981) shows that mordenite would be favored by a high pH, particularly if the hydrothermal fluids were relatively impoverished in Na.

The Samos mordenite is unusually low in Na and high in K compared with other mordenite samples reported in the literature. It is not clear whether the initial conversion of glass to smectite and mordenite produced normal Na-rich mordenite, which was then subsequently altered to K-rich mordenite, or whether the first mordenite to form was rich in K. The SEM observations suggest only one period of mordenite formation. The K-enrichment in the pink rhyolite samples (Table 3) may indicate a later K-rich metasomatic event.

The unusual mordenite compositions parallel the relative abundance of Na and K in synchronous lacustrine sediments. They therefore probably reflect the particular composition of hydrothermal waters in the Miocene.

SUMMARY

Mordenite from Miocene rhyolitic tuffs in Samos is unusually rich in K and depleted in Na. Nevertheless, the XRD pattern is similar to those published for mordenite, and the calculated cell dimensions agree with the relationship between the *b* cell dimension and Si/(Al + Si) found by Passaglia (1975). This unusual mordenite may have formed by hydrothermal circulation of alkaline lake waters, rich in Ca and K, through the volcanic pile.

ACKNOWLEDGMENTS

This work was supported partly by the Natural Sciences and Engineering Research Council of Canada operating grant to G. Pe-Piper. The whole rock analyses were carried out at the Regional Geochemical Centre at Saint Mary's University. Microprobe analyses were made at the Regional Microprobe Centre at Dalhousie University. We thank P. Stoffyn of the Atlantic Geoscience Centre (Bedford Institute of Oceanography) for her help with the SEM and some of the XRD data, D. J. W. Piper for field assistance, and R. A. Sheppard and an anonymous referee for their helpful comments on the manuscript.

REFERENCES

Abbey, S. (1983) Studies in "Standard Samples" of silicate rocks and minerals, 1969–1982: *Geol. Surv. Canada Pap.* **83-15,** 114 pp.

Appleman, D. E. and Evans, H. T., Jr. (1973) Job 9214: Indexing and least squares refinement of powder diffraction data: *U.S. Dept. Commerce, NTIS Doc.* **PB-216188,** 26 pp.

Barrer, R. M. (1948) Syntheses and reactions of mordenite: *J. Chem. Soc.,* 2158–2163.

Barrer, R. M. (1982) *Hydrothermal Chemistry of Zeolites:* Academic Press, London, 360 pp.

Barth-Wirsching, U. and Höller, H. (1989) Experimental studies on zeolite formation conditions: *Eur. J. Mineral.* **1,** 489–506.

Fytikas, M., Innocenti, P., Mazzuoli, R., Peccerillo, A., and Villari, L. (1984) Tertiary to Quaternary evolution of volcanism in the Aegean region: *Geol. Soc. London Special Publ.* **17,** 687–699.

Gottardi, G. and Galli, E. (1985) *Natural Zeolites:* Springer-Verlag, Berlin, 409 pp.

Gude, A. J., 3rd and Sheppard, R. A. (1988) A zeolitic tuff in a lacustrine facies of the Gila conglomerate near Buckhorn, Grant County, New Mexico: *U.S. Geol. Surv. Bull.* **1763,** 22 pp.

Hay, R. L. (1963) Stratigraphy and zeolitic diagenesis of the John Day Formation of Oregon: *Univ. California Publ. Geol. Sci.* **42,** 199–262.

Hawkins, D. B., Sheppard, R. A., and Gude, A. J., 3rd (1978) Hydrothermal systhesis of clinoptilolite and comments on the assemblage phillipsite-clinoptilolite-mordenite: in *Natural Zeolites: Occurrence, Properties, Use,* L. B. Sand and F. A. Mumpton, eds., Pergamon Press, Elmsford, New York, 337–343.

Hemley, J. J. (1962) Alteration studies in the systems Na_2O-Al_2O_3-SiO_2-H_2O and K_2O-Al_2O_3-SiO_2-H_2O: *Geol. Soc. Amer. Abstracts for 1961, Geol. Soc. Amer. Spec. Paper* **68,** 196.

Kirov, G. N., Pechigargov, V., and Landzheva, E. (1979) Experimental crystallization of volcanic glasses in a thermal gradient field: *Chemical Geol.* **26,** 17–28.

Kusakabe, H., Minato, H., Utada, M., and Yamanaka, T. (1981) Phase relations of clinoptilolite, mordenite, analcime, and albite with increasing pH, sodium ion concentration, and temperature: *Univ. Tokyo Sci. Papers, College of General Education* **31,** 39–59.

Maglione, G. and Tardy, Y. (1971) Néoformation pédogénétique d'une zeolite, Ca mordenite, associée aux carbonates de sodium dans une dépression interdunaire des bords du lac Tschad: *C.R. Acad. Sci. Paris ser. D* **272,** 772–774.

Mariner, R. H. and Surdam, R. C. (1970) Alkalinity and formation of zeolites in saline alkaline lakes: *Science* **170,** 977–980.

Meissner, B. (1976) Das Neogen von Ost-Samos, Sedimentationsgeschichte und Korrelation: *Neues Jahrb. Geol. Palaont. Abh.* **152,** 161–176.

Nakajima, W. (1973) Mordenite solid solution in the system $Na_2Al_2Si_{10}O_{24}$-$CaAl_2Si_{10}O_{24}$-H_2O: *Bull. Fac. Educ. Kobe Univ.* **48,** 91–98.

Passaglia, E. (1975) The crystal chemistry of mordenites: *Contrib. Mineral. Petrol.* **50,** 65–77.

Phillips, L. V. (1983) Mordenite occurrences in the Marysvale area, Piute County, Utah: A field and experimental study: *Brigham Young Univ. Geol. Studies* **30,** 95–111.

Seki, Y. (1973) Ionic substitution and stability of mordenite: *J. Geol. Soc. Japan* **79,** 669–676.

Senderov, E. E. (1963) Crystallization of mordenite under hydrothermal conditions: *Geochemistry* (translation from the Russian of "Geochimia") **9,** 848–859.

Sheppard, R. A. and Gude, A. J., 3rd (1965) Zeolitic authigenesis of tuffs in the Ricardo Formation, Kern County, southern California: in *Geol. Surv. Res. 1965, U. S. Geol. Surv. Prof. Pap.* **525-D,** D44–D47.

Sheppard, R. A., Gude, A. J., 3rd, and Fitzpatrick, J. J. (1988) Distribution, characterization, and genesis of mordenite in Miocene tuffs at Yucca Mountain, Nye County, Nevada: *U.S. Geol. Surv. Bull.* **1777,** 22 pp.

Stamatakis, M. (1989a) Authigenic silicates and silica polymorphs in the Miocene saline-alkaline deposits of the Karlovassi Basin, Samos, Greece: *Econ. Geol.* **84,** 788–798.

Stamatakis, M. (1989b) A boron-bearing potassium feldspar in volcanic ash and tuffaceous rocks from Miocene lake deposits, Samos Island, Greece: *Amer. Mineral.* **74,** 230–235.

Stamatakis, M. and Zagouroglou, K. (1984) On the occurrence of niter in the Samos Island: *Mineral Wealth* **33,** 17–26.

Whittemore, O. J. (1972) Synthesis of siliceous mordenites: *Amer. Mineral.* **57,** 1146–1151.

Wirsching, U. (1976) Experiments on hydrothermal alteration processes of rhyolitic glass in closed and "open" system: *Neues Jahrb. Mineralogie, Monatshefte* **5,** 203–213.

(Received 9 May 1990; accepted 25 November 1990; Ms. 2005)